Journal of Experimental Botany, Vol. 70, No. 4 pp. 1375–1388, 2019
doi:10.1093/jxb/ery457 Advance Access Publication 24 January 2019
This paper is available online free of all access charges (see https://academic.oup.com/jxb/pages/openaccess for further details)

RESEARCH PAPER

The Arabidopsis *AMOT1/EIN3* gene plays an important role in the amelioration of ammonium toxicity

Guangjie Li[1,*,†], Lin Zhang[1,2,†], Meng Wang[1], Dongwei Di[1], Herbert J. Kronzucker[3] and Weiming Shi[1,*]

[1] State Key Laboratory of Soil and Sustainable Agriculture, Institute of Soil Science, Chinese Academy of Sciences, No. 71 East Beijing Road, Nanjing 210008, China
[2] University of the Chinese Academy of Sciences, No. 19(A) Yuquan Road, Shijingshan District, Beijing 100049, China
[3] School of Agriculture and Food, Faculty of Veterinary and Agricultural Sciences, The University of Melbourne, Parkville, VIC 3010, Australia

* Correspondence: gjli@issas.ac.cn or wmshi@issas.ac.cn
† These authors contributed equally to this work.

Received 22 September 2018; Editorial decision 18 December 2018; Accepted 19 December 2018

Editor: Christine Foyer, Leeds University, UK

Abstract

Ammonium (NH_4^+) toxicity inhibits shoot growth in Arabidopsis, but the underlying mechanisms remain poorly characterized. Here, we show that a novel Arabidopsis mutant, *ammonium tolerance 1* (*amot1*), exhibits enhanced shoot growth tolerance to NH_4^+. Molecular cloning revealed that *amot1* is a new allele of *EIN3*, a key regulator of ethylene responses. The *amot1* mutant and the allelic *ein3-1* mutants show greater NH_4^+ tolerance than the wild type. Moreover, transgenic plants overexpressing *EIN3* (*EIN3ox*) are more sensitive to NH_4^+ toxicity The ethylene precursor 1-aminocyclopropane-1-carboxylic acid (ACC) increases shoot sensitivity to NH_4^+, whereas the ethylene perception inhibitor Ag^+ decreases sensitivity. NH_4^+ induces ACC and ethylene accumulation. Furthermore, ethylene-insensitive mutants such as *etr1-3* and *ein3eil1* display enhanced NH_4^+ tolerance. In contrast, the ethylene overproduction mutant *eto1-1* exhibits decreased ammonium tolerance. AMOT1/EIN3 positively regulates shoot ROS accumulation, leading to oxidative stress under NH_4^+ stress, a trait that may be related to increased expression of peroxidase-encoding genes. These findings demonstrate the role of *AMOT1/EIN3* in NH_4^+ tolerance and confirm the strong link between NH_4^+ toxicity symptoms and the accumulation of hydrogen peroxide.

Keywords: Ammonium stress, *amot1* mutant, Arabidopsis, AMOT1/EIN3, H_2O_2, peroxidases.

Introduction

Ammonium (NH_4^+), an important source of nitrogen for many species (Kronzucker *et al.*, 1997; Balkos *et al.*, 2010), is frequently present in soils and in the atmosphere in significant quantities (Britto and Kronzucker, 2002; Dupre *et al.*, 2009). However, NH_4^+ is toxic at moderate levels, frequently achieved in soils, to most plants, in particular those used in temperate agriculture, with stunted root and leaf growth as major symptoms of toxicity (Britto and Kronzucker, 2002; Coskun *et al.*, 2013). Several important physiological processes have been linked to excessive NH_4^+ exposure, such as ionic imbalance, relationships with carbon biochemistry, energy consumption, and modifications of hormonal balance (Britto and Kronzucker, 2002; Coskun *et al.*, 2013). Ethylene production has been shown to increase linearly with tissue NH_4^+ accumulation (Barker,

1999a), concurrent with the development of toxicity symptoms (You and Barker, 2002, 2005). In addition, the application of ethylene synthesis and ethylene action inhibitors can ameliorate NH_4^+ toxicity symptoms (Barker and Corey, 1991; Feng and Barker, 1992a, b; You and Barker, 2005; G. Li *et al.*, 2013). Ethylene is synthesized from *S*-adenosyl-L-methionine (SAM) via 1-aminocyclopropane-1-carboxylic acid (ACC). The rate-limiting step in ethylene biosynthesis lies in ACC production via ACC synthase (ACS), followed by ACC conversion to ethylene by ACC oxidase (ACO) (Adams and Yang, 1979). ACS and ACO are encoded by multigene families and are regulated by both developmental and environmental factors. Evolution of ethylene in response to biotic and abiotic stress resulting from ACS and ACO up-regulation is a common phenomenon (Yamagami *et al.*, 2003; Schellingen *et al.*, 2014). In Arabidopsis, the downstream component of the ethylene signaling pathway includes ethylene receptor ETRs (e.g. ETR1), CTR1 (constitutive triple response 1), EIN2 (ethylene-insensitive 2), EIN3/EIL (ethylene-insensitive 3/EIN3-like1), and ERF1 (ethylene-response factor 1) transcription factors (Lei *et al.*, 2011). Ethylene signaling is transduced into the nucleus to cause the accumulation of two master transcriptional activators EIN3 and EIL1, which initiate transcriptional re-programming in various ethylene responses (Yoo *et al.*, 2009; Tao *et al.*, 2015). However, the detailed mechanisms of ethylene biosynthesis and signaling in NH_4^+ stress responses remain unclear.

Reactive oxygen species (ROS) are induced under a wide range of environmental stresses; they can cause oxidative damage leading to injury and death, depending on cellular concentrations. NH_4^+ was found to induce higher levels of H_2O_2 and oxidative stress response reactions in leaves of the aquatic plant *Vallisneria natans* (Wang *et al.*, 2008), Arabidopsis (Podgórska *et al.*, 2013), and other species (Podgórska and Szal, 2015). However, data regarding the pathways involved in NH_4^+ regulation of H_2O_2 production are still rare. ROS can be generated in the apoplast via the activity of NADPH oxidases under stress (Mittler *et al.*, 2004). A group of NADPH oxidases and respiratory burst oxidase homologs (RBOHs) have been identified in Arabidopsis (Sagi and Fluhr, 2006). ROS are tightly regulated via a production/scavenging equilibrium. The expression of genes involved in the ROS regulatory network, including *APX1* (ascorbate peroxidase 1) and *CAT1* (catalase 1) in Arabidopsis (Davletova *et al.*, 2005; Xing *et al.*, 2008), also affects ROS levels. Peroxidases (PODs) have been proposed as alternative producers of ROS (Apel and Hirt, 2004; Bindschedler *et al.*, 2006). PODs catalyze the oxidoreduction of various substrates using H_2O_2. PODs, rather than NADPH oxidase, have been proposed as the major ROS producer in French bean (*Phaseolus vulgaris*) treated with a cell wall elicitor of *Colletotrichum lindemuthianum*, the fungus that causes anthracnose (Bolwell *et al.*, 1998). Kim *et al.* (2010) found that a POD contributes to ROS production during the Arabidopsis root response to potassium deficiency, showing the POD to be a component of the low potassium signal transduction pathway. Recently, Balzergue *et al.* (2017) showed that –Pi induces root tip ROS accumulation, indicating that PODs play a role. Further, the POD inhibitor salicylhydroxamic acid (SHAM) restored root growth and reduced ROS accumulation under –Pi conditions (Balzergue *et al.*, 2017). Although ethylene and ROS have been reported to be involved in NH_4^+ sensitivity, there has been no study to evaluate the role of ethylene in high-NH_4^+-induced ROS production in leaves, and further research is necessary to clarify the circumstances under which NH_4^+ causes oxidative stress in plants.

One approach to elucidating mechanisms of NH_4^+ toxicity in plants is to use mutant lines. Qin *et al.* (2008) isolated the first NH_4^+-sensitive root elongation mutant, *vtc1* (vitamin C defective 1), disrupted in GDP-mannose pyrophosphorylase (GMPase). Recently, several genetic regulators controlling root sensitivity to NH_4^+ have been identified in Arabidopsis, such as *aux1* (auxin resistant 1) (Cao *et al.*, 1993; Li *et al.*, 2011), *trh1* (tiny root hair 1) (Zou *et al.*, 2012), *dpms1* (dolichol phosphate mannose synthase1) (Jadid *et al.*, 2011), and *gsa1* (gravitropism sensitive to ammonium1) (Zou *et al.*, 2013). Elucidation of the function of these genetic regulators in determining the root sensitivity to NH_4^+ offered insight into the molecular basis of historically described physiological responses to NH_4^+ toxicity. In contrast, the underlying mechanisms of impaired leaf growth under NH_4^+ toxicity are still largely unknown. Reduced shoot biomass and leaf chlorosis are important symptoms (Britto and Kronzucker, 2002). Based on their chlorotic phenotypes, ammonium-overly-sensitive 1 (*amos1*) (B. Li *et al.*, 2012) and *amos2* (G. Li *et al.*, 2012) mutants were recently identified: the *AMOS1* locus is identical to *EGY1* (ethylene-dependent gravitropism-deficient and yellow-green-like protein1), which encodes a membrane-bound, ATP-independent metalloprotease localized to plastids, required for chloroplast biogenesis (Chen *et al.*, 2005). However, the genetic locus responsible for the *amos2* mutation has not been identified. These studies, in combination, provide a significantly improved understanding of the process of NH_4^+ toxicity in plants.

Here, we report a novel *Arabidopsis thaliana* mutant, *amot1* (ammonium tolerance 1), which displays enhanced shoot growth in response to NH_4^+ stress. Gene cloning shows *amot1* to be allelic to *EIN3*. Our results demonstrate that the disruption of AMOT1/EIN3 reduces high-NH_4^+-induced ROS accumulation in leaves, leading to reduced oxidative stress in the shoot. Moreover, AMOT1/EIN3 up-regulates shoot expression of the genes coding for PODs, previously shown to correlate positively with NH_4^+-induced changes in ROS content and cell growth inhibition.

Materials and methods

Plant materials and growth conditions

Plant materials used in this work included wild-type (WT) *A. thaliana* L. (Col-0 ecotype) and genetic mutants derived from the Col-0 background. The mutants *ein3-1* (Chao *et al.*, 1997), *eil1-1* (Alonso *et al.*, 2003), *ein3-1eil1-1* (Alonso *et al.*, 2003), *EIN3ox* (*35S:EIN3*) (Chao *et al.*, 1997), and *5×EBS:GUS*/Col-0 transgenic plants (He *et al.*, 2011) were described previously. The *eto1-1* (Alonso and Stepanova, 2004), *etr1-3* (Guzmán and Ecker, 1990), and *rbohd* mutants were obtained from the Arabidopsis Biological Resource Center (ABRC). Seeds were surface-sterilized and cold-treated at 4 °C for 48 h prior to being sown onto standard growth medium. The standard growth medium was described previously (G. Li *et al.*, 2013) and was composed of 2 mM KH_2PO_4, 5 mM $NaNO_3$, 2 mM $MgSO_4$, 1 mM $CaCl_2$, 0.1 mM Fe-EDTA, 50 μM

H_3BO_3, 12 μM $MnSO_4$, 1 μM $ZnCl_2$, 1 μM $CuSO_4$, 0.2 μM Na_2MoO_4, 0.5 g l^{-1} MES, 1% sucrose, and 0.8% agarose (pH 5.7, adjusted with 1 M NaOH). The day of sowing was considered day 0. Seedlings were grown, oriented vertically on the surface of the medium in a growth chamber, under a 16 h light/8 h dark photoperiod, an irradiance of 100 μmol m^{-2} s^{-1}, and a constant temperature of 23±1 °C. Other chemical treatments were provided as additions to the growth medium, as indicated.

Screening conditions

Transfer DNA (T-DNA) lines were constructed in the laboratories of D. Weigel and C. Somerville using the pSKI15 vector. Approximately 7500 independent lines (stock no. N21995) were provided by the ABRC. After surface sterilization, seeds were sown and grown on vertically oriented growth medium plates. After 5 d, seedlings were transferred to growth medium plates supplemented with 20 mM $(NH_4)_2SO_4$. Potential NH_4^+ tolerance mutants were selected after 6 d and rescued, transferred to soil, and allowed to self-fertilize. The homozygous M_4 *amot1* mutant was backcrossed to the WT Col-0, and the resulting F_1 generation was crossed with WT Col-0 twice to remove unlinked mutations caused by the mutagenesis.

Thermal asymmetric interlaced PCR

DNA for PCR amplification was extracted according to Weigel and Glazebrook (2002). Plant T-DNA-flanking sequences were amplified by PCR according to the protocols of Rodrigues *et al.* (2009).

The following primers were used: SKI1, 5'-AATTGGTAATTACTCTTTCTTTTCCTCCATATTGA-3'; SKI2, 5'-ATATTGACCATCATACTCATTGCTGATCCAT-3'; SKI3, 5'-TGATCCATGTAGATTTCCCGGACATGAA-3'; AD1, 5'-TG(AT)G(ACGT)AG(GC)A(ACGT)CA(GC)AGA-3'; AD2, 5'-(ACGT)TCGA(GC)T(AT)T(GC)G(AT)GTT-3'; AD3, 5'-(ACGT)GTCGA(GC)(AT)GA(ACGT)A(AT)GAA-3'; AD4, 5'-AG(AT)-G(ACGT)AG(AT)A(ACGT)CA(AT)AGG-3'; AD5, 5'-(AT)GTG(ACGT)AG-(AT)A(ACGT)CA(ACGT)AGA-3'; and AD6, 5'-(GC)TTG(ACGT)TA(GC)T-(ACGT)CT(ACGT)TGC-3'.

Growth assays

For high-NH_4^+ stress experiments, 5-day-old seedlings were transferred onto growth medium containing various concentrations of $(NH_4)_2SO_4$. Following 6 d of treatment, photographs were taken, and relative rosette size and shoot biomass were measured. To study the effect of precursors or inhibitors, the medium was supplemented with NH_4^+ plus the indicated concentrations of ACC (Sigma), $AgNO_3$ (Shanghai yuanye biotechnology Co. Ltd, Shanghai, China), H_2O_2 (Shanghai yuanye biotechnology Co. Ltd), or SHAM (Shanghai yuanye biotechnology Co. Ltd). The ratio of average rosette size on NH_4^+-stressed plates to the average rosette size on control plates was calculated as relative rosette size, according to Lei *et al.* (2011). The fresh weight of each individual shoot was measured immediately after harvest using a high-precision balance (0.000001) (XP105, Mettler Toledo).

NH_4^+, H_2O_2, MDA, and ACC content, and peroxidase and glutamine synthetase activity assay

Shoots (30–50 mg FW) of each sample were washed with 10 mM $CaSO_4$, frozen in liquid nitrogen, and then extracted with 1 ml of 10 mM formic acid for the NH_4^+ content assay by HPLC, following derivatization with *o*-phthaldialdehyde (Sigma) as described previously (G. Li *et al.*, 2012). H_2O_2 content was determined by the POD-coupled assay according to Veljovic-Jovanovic *et al.* (2002). Arabidopsis shoots were ground in liquid nitrogen, and the powder was extracted in 2 ml of 1 M $HClO_4$ in the presence of insoluble polyvinylpyrrolidone (5%). The homogenate was centrifuged at 12 000 *g* for 10 min, and the supernatant was neutralized with 5 M K_2CO_3 to pH 5.6 in the presence of 100 ml of 0.3 M phosphate buffer (pH 5.6). The solution was centrifuged at 12 000 *g* for 1 min, and the sample was incubated for 10 min with 1 U of ascorbate oxidase (Shanghai yuanye biotechnology Co. Ltd) to oxidize ascorbate prior to use in the assay. The reaction mixture consisted of 0.1 M phosphate buffer (pH 6.5), 3.3 mM DMAB (Shanghai yuanye biotechnology Co. Ltd), 0.07 mM MBTH (Shanghai yuanye biotechnology Co. Ltd), and 0.3 U of POD (Shanghai yuanye biotechnology Co. Ltd). The reaction was initiated by the addition of the sample. The absorbance change at 590 nm was monitored at 25 °C. The malondialdehyde (MDA) level was measured using a thiobarbituric acid-reactive substance (TBARS) assay kit (Nanjing Jiancheng Bioengineering Institute, Nanjing, China) (Ren *et al.*, 2015). Shoot ACC content was detected by negative ion chemical ionization (NICI) GC-MS (Schellingen *et al.*, 2014). Data are expressed in nmol g^{-1} FW. POD activity was detected by a micro-POD assay kit (BC0095, Solarbio, Beijing, China) according to the manufacturer's recommendations. POD activity is expressed as U mg^{-1} based on protein content. Glutamine synthetase (GS) activity was detected by a GS kit (BC0910, Solarbio) (Zhao *et al.*, 2017). The specific enzyme activity (U g^{-1} FW) was defined as the amount of enzyme units catalyzing the transformation of 1 μM substrate per minute by the amount of fresh weight in grams.

Real-time quantitative PCR analysis

Total RNA was extracted from Arabidopsis shoots. Gene sequences were provided by the National Center of Biotechnology Information (NCBI), and gene-specific primers for real-time quantitative PCR (qRT-PCR) were designed using Primer-5 software (see Supplementary Table S1 at *JXB* online). *CBP20* (nuclear-encoded cap-binding protein) and *ACTIN2* were used as the internal reference genes, and relative RNA abundance was normalized to the *CBP20* or *ACTIN2* internal control ($[mRNA]_{gene}/[mRNA]_{CBP20}$ or $[mRNA]_{gene}/[mRNA]_{ACTIN2}$).

Histochemical staining and image analysis

Histochemical staining of H_2O_2 was performed as previously described (Dong *et al.*, 2009) with minor modifications. Shoots were vacuum-infiltrated with 0.1 mg ml^{-1} 3,3′-diaminobenzidine (DAB) in 50 mM Tris-acetate buffer, at pH 5.0. Samples were incubated for 24 h at room temperature in the dark prior to transfer to 80% ethanol. Histochemical analysis of β-glucuronidase (GUS) reporter enzyme activity was performed as described by Weigel and Glazebrook (2002). GUS or H_2O_2 staining in the shoot was carried out using an Olympus SZX10 stereo microscope. Intensities of the GUS- and DAB-stained zone were quantified using Image-J software. All staining and image analysis procedures were repeated at least twice.

Ethylene measurements

After seedling exposure to 40 mM NH_4^+ for varying durations, as indicated, shoots from the control and treatments were weighed and put into 5 ml gas-tight vials containing 1 ml of agar medium (0.7% agar). Headspace samples (1 ml) were withdrawn and analyzed using a GC-6850 gas chromatograph (Agilent Technologies Japan, Ltd), which was equipped with an FID detector.

Yeast one-hybrid (Y1H) analysis

Promoter fragments from At1g49570 (2217 bp) and At5g19890 (1692 bp) were cloned into the pAbAi vector to produce the bait constructs pAbAi-At1g49570 and pAbAi-At5g19890, respectively. The coding seuqence (CDS) of *AMOT1/EIN3* was fused to the pGADT7 vector to generate a prey construct, AD-*EIN3*. The bait construct and the empty vector (AD) served as the negative control; p53-AbAi/pGAD-p53 were used as a positive control and transformed separately into yeast cells. Transformed yeast cells were diluted with a 10× dilution series and dotted onto SD plates lacking Ura and Leu (with or without antibiotic).

Statistical and graphical analyses

For all experiments, data were statistically analyzed using the SPSS 13.0 program (SPSS Chicago, IL, USA). Details are shown in the figure legends. Graphs were produced using Origin 8.0. All graphs and images were arranged using Adobe Photoshop 7.0.

Results

Enhanced tolerance of the amot1 *mutant to ammonium toxicity*

Under our growth conditions, NH_4^+, at concentrations of 20–30 mM, caused slight reductions in shoot size and biomass (Supplementary Fig. S1). A concentration of 40 mM significantly inhibited shoot size and biomass (Supplementary Fig. S1). To explore the mechanisms of NH_4^+-induced shoot growth inhibition, we performed a forward genetic screen for seedlings that show a shoot phenotype that was more resistant than WT plants when grown on medium containing 40 mM NH_4^+. Seedlings that appeared similar to the WT without NH_4^+ but displayed significantly higher resistance of shoot growth to NH_4^+ were *amot* (ammonium tolerance) mutants. We present the characterization of the *amot1* mutant.

In agar plates without NH_4^+, the *amot1* shoot growth phenotype was indistinguishable from that of the WT (Fig. 1A). However, when grown in the presence of high NH_4^+, *amot1* shoot growth displayed greater resistance to NH_4^+ than the WT (Fig. 1A).

NH_4^+-treated WT and *amot1* plants showed a dose-dependent inhibitory effect of NH_4^+ on the growth of aerial parts in response to a range of NH_4^+ concentrations, but WT shoot growth was inhibited more than in *amot1* at the concentrations used (Fig. 1B, C). Furthermore, we analyzed the shoot phenotypes of *amot1* and WT seedlings in response to 40 mM NH_4^+ over time. The shoot growth between WT and *amot1* seedlings remained similar 2 d after NH_4^+ addition, but the difference was clearly accentuated under prolonged NH_4^+ treatment, with the mutant maintaining significantly higher growth rates (Fig. 1D, E). Considering these results together, *amot1* emerges as the first NH_4^+-resistant mutant, displaying superior shoot growth.

The WT and *amot1* seedlings were also treated on medium enriched with a variety of ions and molecules, and the results indicate that *amot1* seedlings are highly resistant to both $(NH_4)_2SO_4$ and NH_4Cl, but responded to 15 mM and 20 mM K_2SO_4 or 60 mM and 80 mM mannitol in a similar pattern to the WT (Fig. 2).

The amot1 *mutant is a novel* ein3 *allele, and loss of* EIN3 *function enhances ammonium tolerance*

The WT as female parent was crossed with the homozygous mutant as the pollen donor. F_1 plants were selfed to obtain

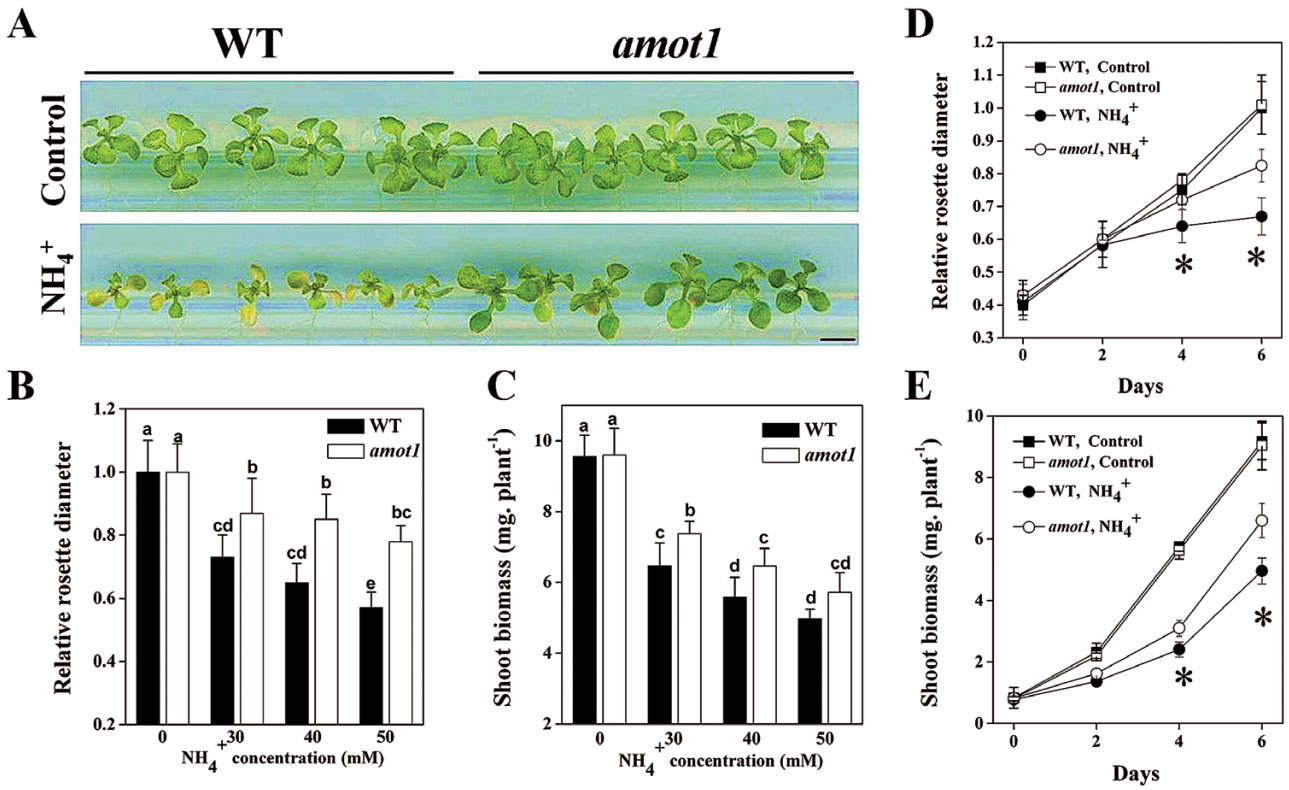

Fig. 1. Isolation and characterization of the ammonium-tolerant *amot1* mutant. (A) Appearance of *Arabidopsis thaliana* wild-type (WT) and *amot1* mutant plants following treatment with NH_4^+. Five-day-old plants were transferred to control and 40 mM NH_4^+ concentration for 6 d, and then pictures were taken. Scale bars=0.5 cm. (B and C) Relative rosette diameter and fresh shoot weight of *A. thaliana* WT and *amot1* mutant plants following treatment with various NH_4^+ concentrations for 6 d. The rosette diameter on control nutrient solution was considered as 1. Values are the means ±SD, n=8–11. Different letters indicate statistical differences at $P<0.05$ (one-way ANOVA with Duncan post-hoc test). (D and E) Relative rosette diameter and fresh shoot weight of *A. thaliana* WT and *amot1* mutant plants following treatment with 40 mM NH_4^+ for 0, 2, 4, and 6 d. Values are the means ±SD, n=6–10. Asterisks indicate statistical differences between the WT and *amot1* under NH_4^+ treatment at the indicated times (independent samples t-test, $^*P<0.05$). (This figure is available in color at *JXB* online.)

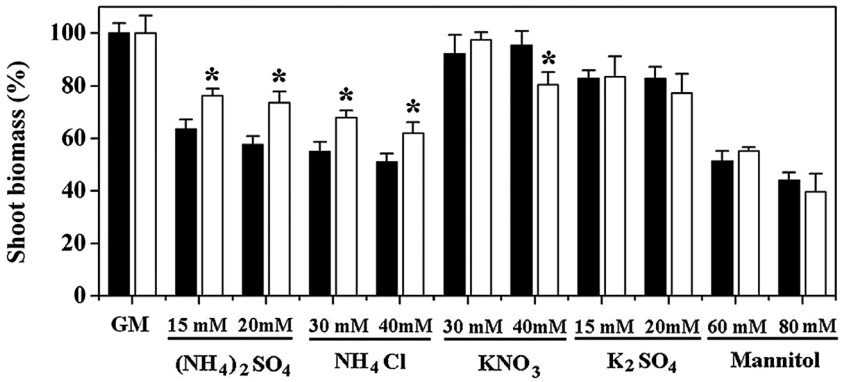

Fig. 2. Specificity of the *amot1* mutant to NH_4^+. WT and *amot1* seedlings were grown for 5 d on growth medium (GM) and then transferred to medium supplemented with salts and osmotica as indicated. Shoot fresh weight was measured 6 d after transfer. Growth on control nutrient (GM) was considered as 100%. Values are the means ±SD, n=10–14. Asterisks indicate statistical differences between the mutant and WT (independent samples t-test, $^*P<0.05$).

F_2 seeds. Both F_1 and F_2 seeds were assayed for growth on NH_4^+ medium. All examined F_1 progeny (45 seedlings) displayed the same phenotypes as the WT. In the F_2 population, the *amot1* phenotype segregated at an approximate 1:3 ratio (*amot1*:WT=54:142; x^2=0.55, P>0.05), indicating that *amot1* is a recessive mutation at a single nuclear locus. T-DNA-flanking sequences were isolated from the mutant by thermal asymmetric interlaced PCR, and sequence analysis revealed that the pSKI15 T-DNA was inserted into the exon of the *EIN3* gene (At3g20770) in *amot1*, 192 bp downstream of the start codon, ATG [Fig. 3A(a)]. *EIN3* gene transcripts were greatly reduced in *amot1* compared with the WT [Fig. 3A(b) and (c)]. To ascertain further whether the NH_4^+-resistant phenotype in *amot1* is due to the mutation in the *EIN3* gene, we analyzed the previously reported allele *ein3-1* (Chao *et al.*, 1997) and crossed the *amot1* mutant with *ein3-1* plants. With exposure to 40 mM NH_4^+, shoot size and biomass in *ein3-1* seedlings were indeed similar to those of *amot1* seedlings (Fig. 3B). Furthermore, the *amot1* mutant was crossed to *ein3-1*, and the F_1 progeny showed a phenotype similar to that of the parents in the presence of NH_4^+ (Fig. 3B). Collectively, these results show that the *amot1* mutant is a new loss-of-function allele of the *EIN3* gene.

AMOT1/EIN3 is a member of a protein family that includes EIN3-like (EIL) proteins (Chao *et al.*, 1997) and initiates transcriptional re-programming in various ethylene responses (Guo and Ecker, 2004; Peng *et al.*, 2014). We sought to determine the role of AMOT1/EIN3 in NH_4^+ resistance. Because AMOT1/EIN3 and its close homolog EIL1 functionally overlap (Chao *et al.*, 1997; An *et al.*, 2010), we examined the *ein3-1eil1-1* double mutant seedling response under various NH_4^+ concentrations. Under high NH_4^+, *ein3-1eil1-1* had superior tolerance to NH_4^+ compared with the WT (26% reduction in *ein3-1eil1-1* versus 52% in the WT at 40 mM NH_4^+) (Fig. 3C). Furthermore, in contrast to the *ein3* single mutant's tolerant phenotype, the *ein3-1eil1-1* double mutant exhibited a more tolerant phenotype than the *amot1* mutant (Fig. 3C). We also examined the phenotype of the *eil1* single mutant upon treatment with high NH_4^+; however, the *eil1-1* mutant was similar to the WT under high NH_4^+ (Supplementary Fig. S2). Next, we examined the NH_4^+-responsive phenotype of a transgenic line overexpressing EIN3 under the control of the 35S promoter (35S:EIN3/*Col-0* or *EIN3ox*), which displays an enhanced ethylene response (Chao *et al.*, 1997; An *et al.*, 2010; Z. Li *et al.*, 2013). The transcripts of *AMOT1/EIN3* were significantly increased in the *EIN3ox* seedlings [Z. Li *et al.*, 2013; Fig. 3A(b) and (c)]. Under high NH_4^+, *EIN3ox* plants displayed increased sensitivity, based on shoot size and biomass, when compared with their WT counterparts (73% shoot biomass reduction in *EIN3ox* plants versus 52% in the WT at 40 mM NH_4^+) (Fig. 3C). Together, these results suggest that constitutive overexpression of *AMOT1/EIN3* leads to elevated shoot NH_4^+ sensitivity in Arabidopsis. Consistent with a previous report (G. Li *et al.*, 2013), the *ein3eil1* lateral root number was also more resistant than that of the WT to high-NH_4^+ stress (Supplementary Fig. S3).

Enhanced shoot ethylene evolution is involved in ammonium-mediated inhibition of shoot growth

Aerial tissue NH_4^+ content was determined, and the NH_4^+ content increased gradually with treatment time compared with that in untreated shoots (Fig. 4A). Shoot ethylene production under NH_4^+ exposure was also significantly greater than without NH_4^+ and increased linearly with NH_4^+ treatment time (Fig. 4B), consistent with Barker (1999*b*). Ethylene is synthesized from SAM via ACC, which is catalyzed by the enzyme ACS (Adams and Yang, 1979). ACC amounts in untreated and treated seedlings are presented in Fig. 4C. Consistent with previous reports, ACC amounts increased linearly with NH_4^+ treatment time. As ACS and ACO are key enzymes of the ethylene biosynthetic pathway in plants, *AtACS2*, *AtACS7*, *AtACS11*, and *AtACO2* expression was examined. Expression of the four genes was rapidly up-regulated in response to high NH_4^+ (Fig. 4D).

We further investigated the activity of AMOT1/EIN3 in response to NH_4^+ in shoot. A transgenic reporter line harboring the GUS gene driven by five tandem repeats of the EIN3-binding site (EBS) followed by a minimal 35S promoter (*5×EBS:GUS*/Col-0) has been used to monitor the transcriptional activity of EIN3 (Stepanova *et al.*, 2007; He *et al.*, 2011). Following NH_4^+ treatment, GUS staining became intensified in the cotyledons of *5×EBS:GUS*/Col-0 plants (Fig. 4F),

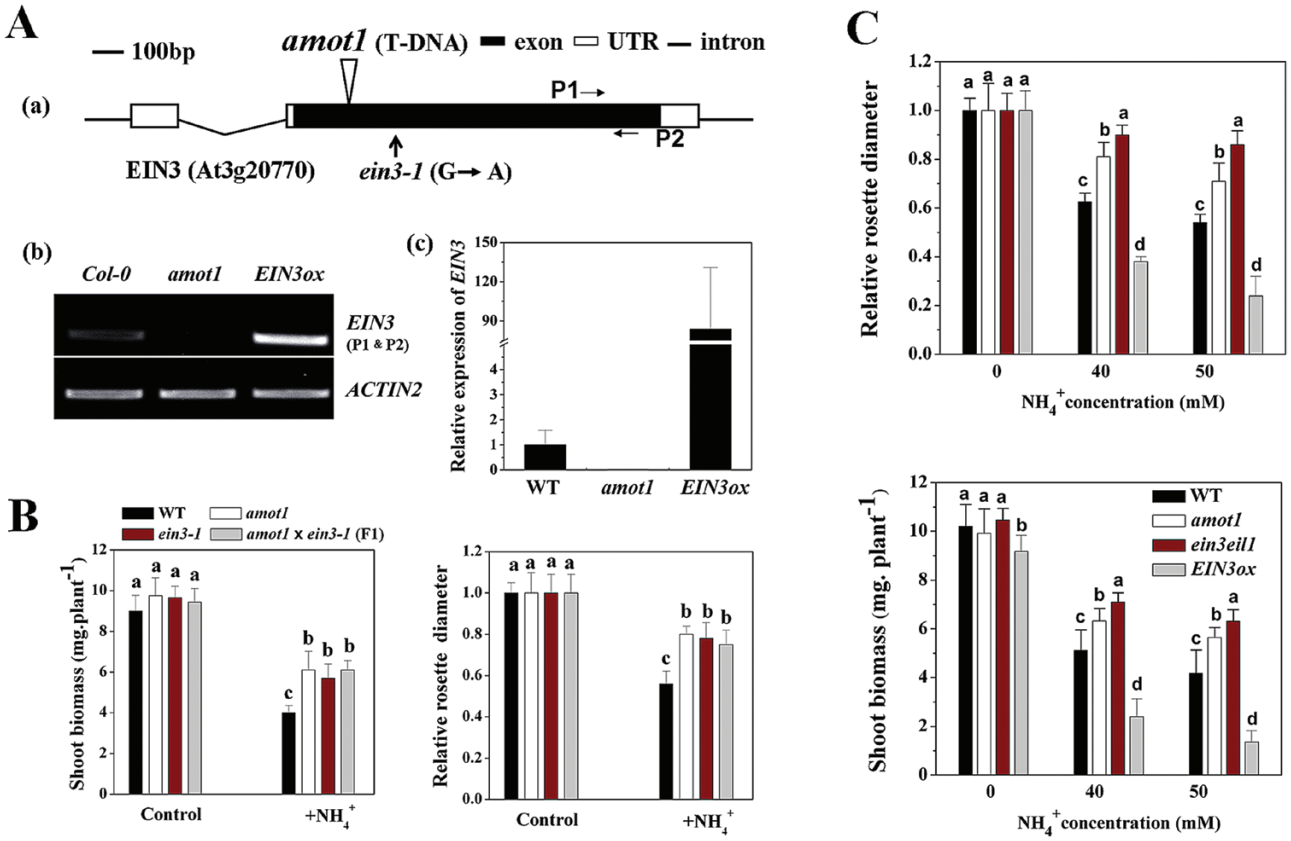

Fig. 3. Molecular characterization of the *Arabidopsis thaliana amot1* mutant. (A) (a) Diagram illustrating the genomic coding sequence of the Arabidopsis *AMOT1/EIN3* gene and the locations of the mutant alleles *amot1* and *ein3-1*. UTR, untranslated region. (b) RT-PCR analysis of *EIN3* transcripts in WT, *EIN3ox*, and the *amot1* mutant plants. The *ACTIN2* gene was used as an internal control. (c) Expression of *EIN3* in WT, *EIN3ox*, and the *amot1* mutant plants analyzed by qRT-PCR analysis. Values are means ±SD of three replicates. *ACTIN2* was used as the internal reference gene, and *EIN3* expression of the WT was considered as 1. (B) *amot1* is allelic to the *ein3-1* mutant. WT, *amot1*, *ein3-1*, and F_1 progeny from crosses between *amot1* and *ein3-1* were grown on 40 mM NH_4^+ for 6 d. The relative rosette diameter on control nutrient solution was considered as 1. Values are the means ±SD, n=7–12. (C) Effect of various NH_4^+ concentrations on relative rosette diameter, and fresh shoot weight of WT, *ein3eil1*, *amot1*, and *EIN3ox* seedlings. Five-day-old plants were transferred to control and 40 mM NH_4^+ concentration for 6 d. Values are the means ±SD, n=5–8. Different letters indicate statistical differences at P<0.05 (one-way ANOVA analysis with Duncan post-hoc test). (This figure is available in color at *JXB* online.)

indicative of elevated levels of AMOT1/EIN3 activity. We also observed that the expression of the ethylene-responsive gene *ERF1* was up-regulated by NH_4^+ in the WT (Fig. 4G). In keeping with the results on AMOT1/EIN3 activity, expression of *ERF1*, a direct target gene of EIN3 (Solano *et al.*, 1998), was also lower in the NH_4^+-treated *ein3eil1* mutant, but higher in *EIN3ox* lines, compared with the WT (Fig. 4G).

The WT plants treated with the ethylene biosynthetic precursor ACC displayed decreased tolerance to NH_4^+ (Fig. 4E). Consistent with this, the ethylene overproduction mutant *eto1-1* (ethylene overproducer 1) also showed reduced NH_4^+ tolerance compared with the WT (Fig. 4H). In the presence of the ethylene receptor antagonist Ag^+, shoot growth of the WT was significantly increased when the plants were exposed to NH_4^+ stress (Fig. 4E). As ethylene is known to activate downstream signaling pathways by binding to ethylene receptors (e.g. ETR1), we examined whether ethylene regulates shoot growth sensitivity to NH_4^+ in such a way. Shoot growth in the ethylene-insensitive (ethylene receptor) mutant *etr1-3* and positive regulator mutants in ethylene signaling, *amot1* and *ein3-1*, was more tolerant to NH_4^+ than that of the WT; consistent with this, *EIN3ox* lines displayed increased shoot growth sensitivity (Fig. 4H). These results indicate that ethylene has a negative effect on NH_4^+ tolerance in Arabidopsis shoot growth.

AMOT1/EIN3 regulates ammonium-induced ROS accumulation in shoots

High NH_4^+ induces an increase in ROS in plants; however, the biological mechanism of NH_4^+-induced ROS accumulation remains largely unknown. Here, we examined the levels of endogenous H_2O_2 in the WT, *ein3eil1*, and *EIN3ox* in response to high-NH_4^+ treatment. NH_4^+ stress increased H_2O_2 accumulation in the cotyledons of the WT, indicated by DAB staining (Fig. 5A, B). We further found higher levels of DAB staining in *EIN3ox* but lower levels in *ein3eil1* than in the WT following NH_4^+ stress (Fig. 5A, B), in accordance with the NH_4^+ tolerance phenotypes of these genotypes (Fig. 3C). We also measured the H_2O_2 contents in shoots. As inferred from DAB staining assays, high-NH_4^+ treatment induced accumulation of H_2O_2 in the WT. However, the level was lower in *ein3eil1* and higher in *EIN3ox* shoots compared with Col-0 under NH_4^+ stress (Fig. 5C). The H_2O_2 content under control conditions was not significantly different among the three ecotypes

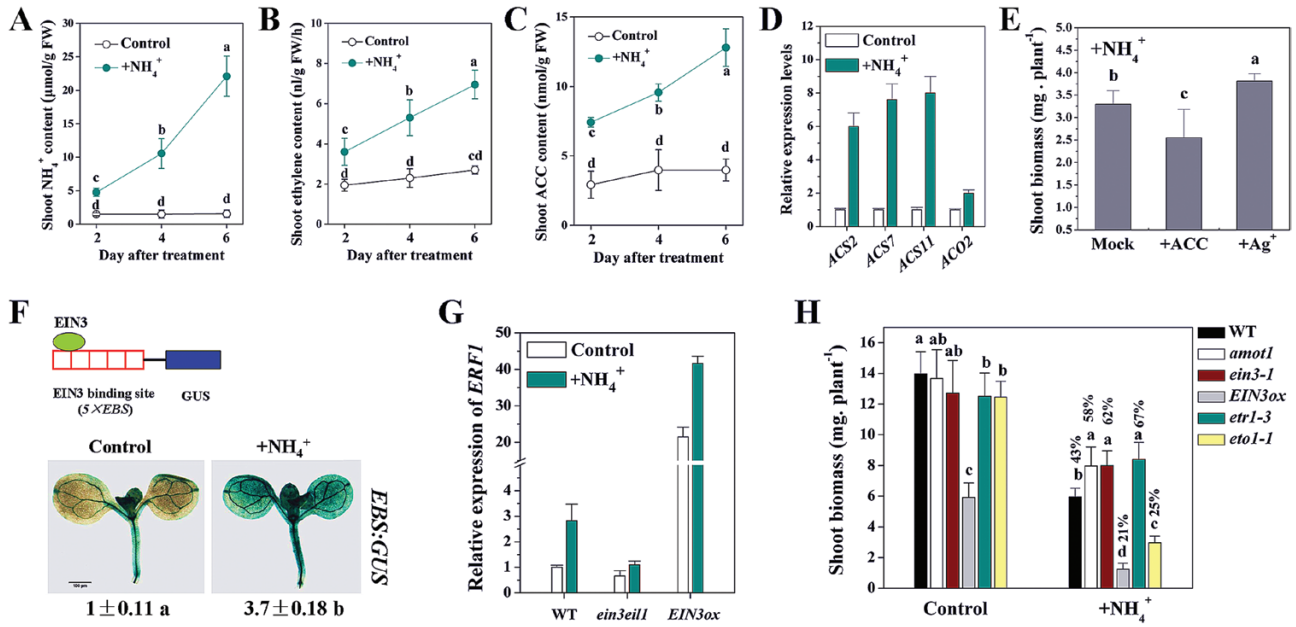

Fig. 4. Effects of ethylene on shoot growth tolerance to NH_4^+. (A) NH_4^+ content in Arabidopsis shoots for the duration of the NH_4^+ treatment. (B) Ethylene evolution in Arabidopsis shoots for the duration of the NH_4^+ treatment. (C) 1-Aminocyclopropane-1-carboxylic acid (ACC) content in Arabidopsis shoots for the duration of the NH_4^+ treatment. Seedlings at 5 d after germination were exposed to NH_4^+ for varying treatment times, and NH_4^+ content (A), ethylene evolution (B), and ACC content were determined. Values are means ±SD of three replicates. Different letters indicate statistical differences at $P<0.05$ (one-way ANOVA with Duncan post-hoc test). (D) Effect of NH_4^+ treatment on shoot *ACS* and *ACO* genes expression by qRT-PCR for 6 h. Values are means ±SD of three replicates. *CBP20* was used as the internal reference gene, and the control was considered as 1. (E) Effect of supplied ethylene inhibitors 30 μM $AgNO_3$ and 25 μM ACC on shoot biomass of WT seedlings grown in 40 mM NH_4^+ treatment medium. Values are the means ±SD, n=10–12. (F) Schematic diagram of the EIN3 activity reporter system showing the EIN3 protein, five tandem repeats of the EBS (*5×EBS*), and the *GUS* gene. Expression of *5×EBS:GUS* in leaves of the WT under control conditions and 24 h NH_4^+ treatment. One representative sample from each treatment (10 plants) is shown. GUS staining intensity was quantified using Image J software, and the control was considered as 1. Values are means ±SD of three replicates. (G) Effect of NH_4^+ treatment on shoot *ERF1* gene expression of WT, *ein3eil1*, and *EIN3ox* lines by qRT-PCR for 6 h. Values are means ±SD of three replicates. *ACTIN2* was used as the internal reference gene, and the WT control was considered as 1. (H) Effect of NH_4^+ treatment for 6 d on shoot fresh weight of WT, *amot1*, *ein3-1*, *EIN3ox*, *etr1-3*, and *eto1-1* seedlings. Values are the means ±SD, n=12. Different letters indicate statistical differences at $P<0.05$ of control and NH_4^+ treatment, respectively (one-way ANOVA with Duncan post-hoc test).

(Supplementary Fig. S4). A split-shoot experiment was devised to examine further the relationship between NH_4^+-induced AMOT1/EIN3 transcriptional activity and ROS accumulation (Supplementary Fig. S5A). The cotyledon supplied with NH_4^+ displayed significantly increased *EBS:GUS* expression compared with the untreated cotyledon (Supplementary Fig. S5B). Consistent with *EBS:GUS* inductive sites, a higher intensity of DAB staining was also detected in the NH_4^+-treated cotyledon (Supplementary Fig. S5C).

In this study, the concentration of MDA equivalents was increased in NH_4^+-treated leaves (Fig. 6A). However, we observed a higher MDA level in *EIN3ox*, and a lower level in *ein3eil1* than in the WT following NH_4^+ stress (Fig. 6A). The effects of NH_4^+ on shoot growth were also examined in combination with external H_2O_2. The combined treatment with NH_4^+ and H_2O_2 in the medium markedly inhibited shoot growth compared with NH_4^+ alone, and the combined treatment inhibited shoot growth more significantly in *amot1* and *ein3eil1* (Fig. 6B).

We further examined the expression of genes encoding antioxidant metabolic enzymes, such as *APX1*, *APX2*, *CAT1*, *CAT2*, and *CAT3*. NH_4^+ stress did not induce *APX* and *CAT* gene expression in WT shoots, and these genes were also not much affected in *ein3eil1* and *EIN3ox* seedlings under NH_4^+ stress (Fig. 6C), suggesting that AMOT1/EIN3 regulation of NH_4^+-induced ROS accumulation might not be related to *APX1*-, *APX2*-, *CAT1*-, *CAT2*-, and *CAT3*-mediated antioxidant activity. Previous studies showed that drought stress increases *RBOH* transcript levels (Lee *et al.*, 2012). However, the expression patterns of RBOHA, RBOHB, RBOHD, and RBOHF under control and high-NH_4^+ stress were similar, and they were also not much affected in the *ein3eil1* mutant and in *EIN3ox* lines compared with the WT (Fig. 6C). Furthermore, DAB staining and shoot growth in response to high-NH_4^+ stress were also similar between the WT and the *rbohd* mutant (Supplementary Fig. S6).

AMOT1/EIN3 induces the transcription of peroxidases and increases their activity

Podgórska *et al.* (2015) proposed that higher POD levels are positively correlated with NH_4^+-induced ROS generation and cell growth inhibition. We found that the expression of two of the genes encoding PODs, At5g19890 and At1g48570, was induced by NH_4^+ treatment in the WT, and expression was more elevated in *EIN3ox* while it was reduced in *ein3eil1* with or without NH_4^+ (Fig. 7A, B). The transcript levels of other POD-encoding genes, such as At5g42180, At2g18980, At4g11290, and At3g49960, were not increased by NH_4^+ treatment in the WT, and were also not significantly altered in *EIN3ox* and *ein3eil1* seedlings, under either normal or NH_4^+

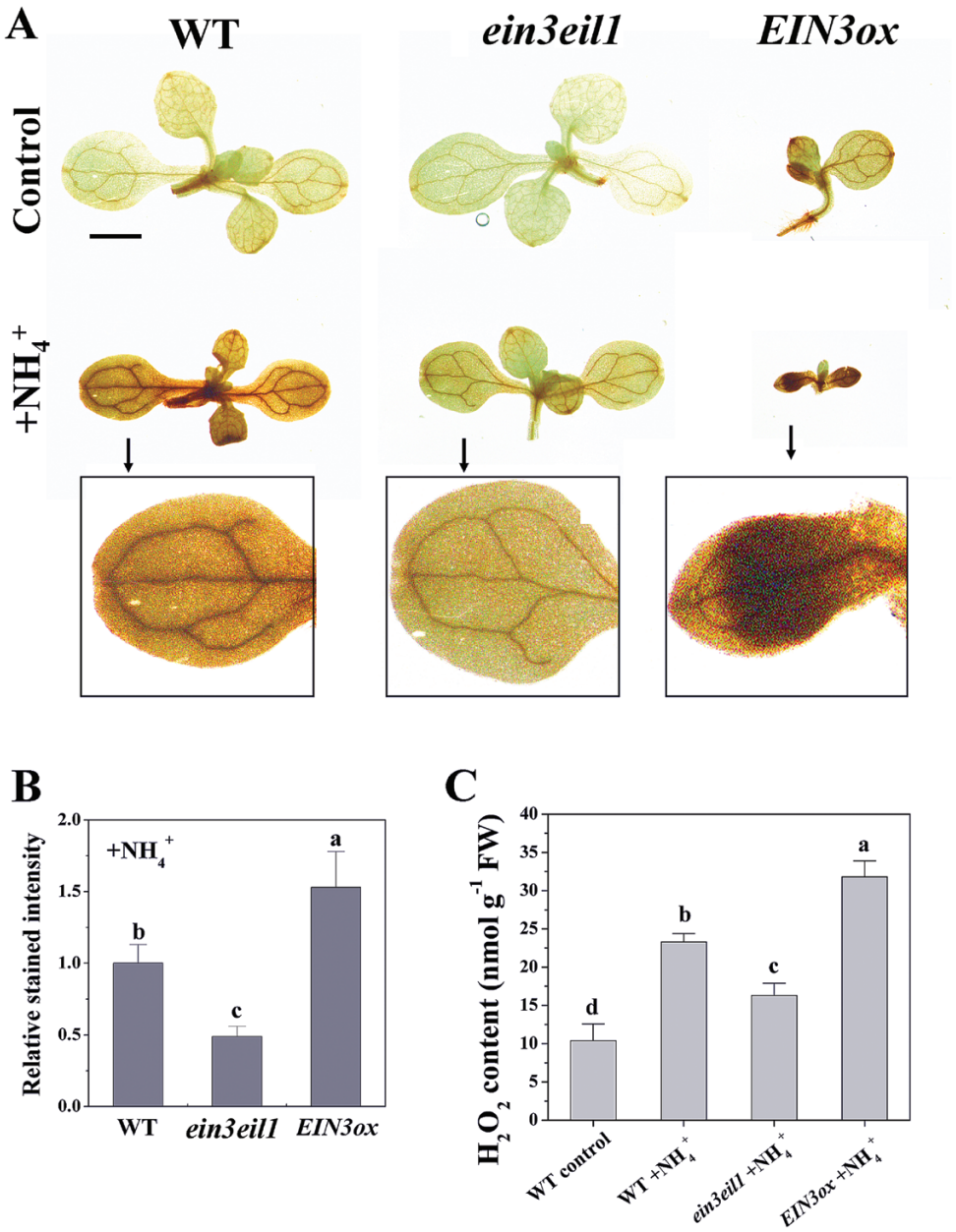

Fig. 5. Effects of EIN3 on NH_4^+-induced H_2O_2 accumulation in shoots. (A) *In situ* detection of WT, *ein3eil1*, and *EIN3ox* leaf H_2O_2. Seedlings at 5 d were exposed to 40 mM NH_4^+ for 3 d, and then DAB staining of shoots was performed. Scale bars=1 mm. The inserts show images of partial enlargement, as indicated by arrows. (B) The mean relative DAB staining intensity in the WT, *ein3eil1*, and *EIN3ox* of the NH_4^+-treated shoots in (A), and the WT was considered as 1. Values are the means ±SD, n=10–15. (C) H_2O_2 concentration in the WT, *EIN3ox*, and *ein3eil1* shoot tissue. Seedlings at 5 d were exposed to 40 mM NH_4^+ for 3 d, and the contents of H_2O_2 were determined as described in the Materials and methods. Values are means ±SD of three replicates. Different letters indicate statistical differences at P<0.05 (one-way ANOVA with Duncan post-hoc test).

stress conditions (Supplementary Fig. S7). The POD activity assay also showed that POD activity was significantly elevated in *EIN3ox* seedlings compared with the WT and *ein3eil1* under NH_4^+ stress (Fig. 7C). POD activity in *EIN3ox* seedlings under control conditions was also slightly elevated compared with the WT and with *ein3eil1* (Supplementary Fig. S8). We next analyzed the promoter regions of two POD genes (At5g19890 and At1g48570) and found EBSs (ATGTA) in each promoter (data not shown). To test the interaction between the AMOT1/EIN3 protein and the At5g19890 and At1g48570 promoters, a Y1H assay was performed. As shown in Fig. 7D, bait yeast cells co-transformed with the empty vector (AD) or the fusion vector (AD-EIN3) grew well on synthetic dropout medium (SD) without Ura and Leu. However, only the yeast cells co-transformed with the fusion vector AD-EIN3 survive on the selective medium supplemented with 400 ng ml^{-1} aureobasidin A (AbA; Fig. 7D). The data suggest that the AMOT1/EIN3 protein interacts with the At5g19890 and At1g48570 promoters in the yeast system. SHAM is a widely used POD inhibitor (Balzergue *et al.*, 2017). The shoot biomass of the WT and *EIN3ox* lines was increased under NH_4^+ stress after SHAM treatment, but no effects on *ein3eil1* lines were observed (Fig. 7E, F). Furthermore, the POD inhibitor SHAM could decrease NH_4^+-induced DAB staining, indicating H_2O_2 accumulation in both WT and *EIN3ox* leaves (Fig. 7G; Supplementary Fig. S9).

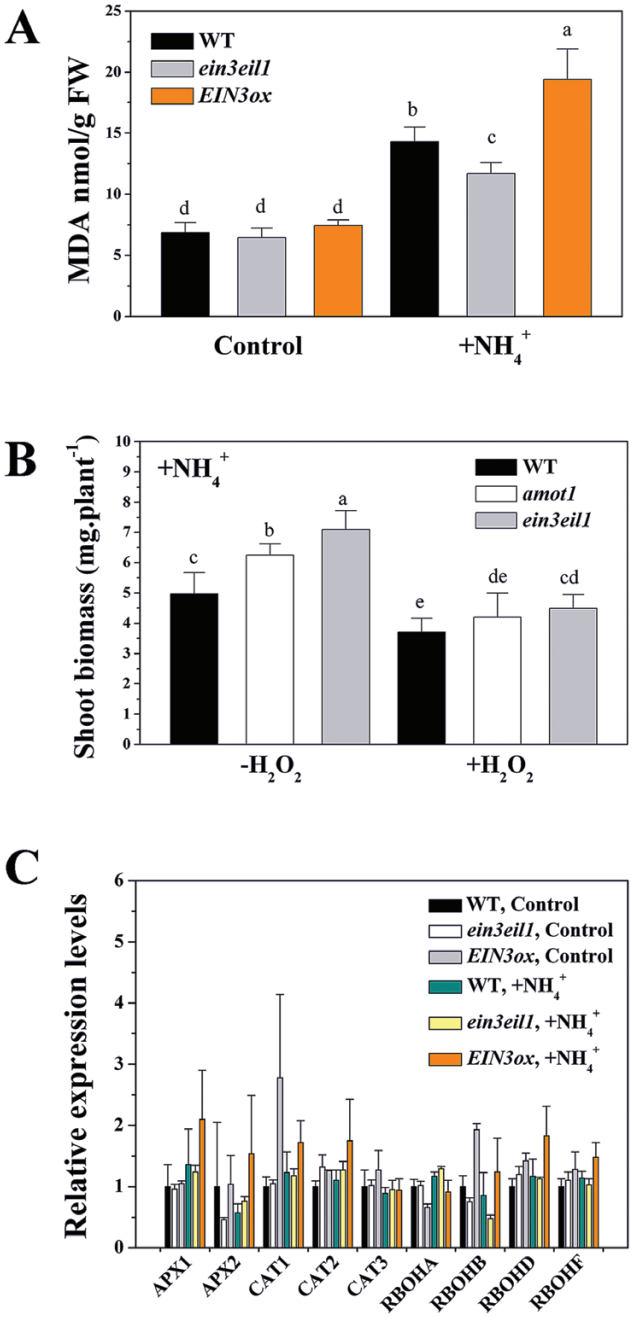

Fig. 6. Effects of EIN3 on NH_4^+-induced lipid peroxidation in shoots and related gene expression. (A) Lipid peroxidation (MDA content) in the WT, *ein3eil1*, and *EIN3ox* shoot tissue. Seedlings at 5 d were exposed to 40 mM NH_4^+ for 6 d. Values are means ±SD of three replicates. (B) Effect of external H_2O_2 on shoot biomass of WT, *ein3eil1*, and *amot1* plants under NH_4^+ treatment. Five-day-old seedlings were transferred to medium supplemented with NH_4^+ alone or in combination with 2 mM H_2O_2 for 6 d. *n*=7–10. (C) Effect of NH_4^+ on gene expression of WT, *EIN3ox*, and *ein3eil1* shoot tissue by qRT-PCR for 6 h. Values are means ±SD of three replicates. *ACTIN2* was used as the internal reference gene, and the WT control was considered as 1. Different letters indicate statistical differences at $P<0.05$ (one-way ANOVA with Duncan post-hoc test).

The amot1 *mutant accumulates less* NH_4^+ *in shoot tissue under* NH_4^+ *toxicity*

There was no difference in shoot NH_4^+ content of the WT, *amot1*, and *ein3eil1* with 3 d of NH_4^+ treatment (Fig. 8A), although ROS accumulation was greater in WT shoots than in those of *ein3eil1* at this treatment time (Fig. 5). However, higher levels of NH_4^+ in the WT, but lower levels in *amot1* and *ein3eil1*, than in the WT were recorded following high-NH_4^+ stress during a 6 d treatment (Fig. 8A). Consistently, NH_4^+ accumulation was slightly higher in *EIN3ox* shoots than in the WT following the treatment (Fig. 8B). Activities of the enzyme GS, centrally involved in the NH_4^+ assimilation process (Kronzucker *et al.*, 1995; Hirano *et al.*, 2008), was determined in shoots of the WT and *amot1*. GS activity was induced by external NH_4^+ in NH_4^+-fed WT and *amot1* plants, but this increase was not significantly different in the two genotypes (Fig.8C). This indicates that NH_4^+ metabolism was not affected by the *AMOT1* mutation.

Discussion

Stunted root system and decreased leaf bomass are among the most visible phenotypic manifestations of NH_4^+ toxicity in higher plants (Britto and Kronzucker, 2002). Several genetic regulators controlling root sensitivity to NH_4^+ have been identified in Arabidopsis (Li *et al.*, 2014); however, little is known about the specific targets and pathways that lead to impaired leaf growth in the context of NH_4^+ toxicity. To gain insight into the mechanisms of the effects of NH_4^+ on shoot growth, we employed a molecular genetics approach, based on a mutant screen for altered response to NH_4^+. In the current work, enhanced NH_4^+ tolerance of shoot growth was found in *amot1*. We further revealed that the nuclear *AMOT1* locus is identical to *EIN3*, which encodes a transcriptional activator required for initiating transcriptional re-programming in various ethylene responses (Guo and Ecker, 2004; Yoo *et al.*, 2009). It was found that *amot1* and *ein3-1*, a reported allele, showed enhanced shoot growth tolerance compared with the WT, but the transgenic line overexpressing EIN3 (*EIN3ox*) was more sensitive. The activity of AMOT1/EIN3, indicated by using *EBS:GUS* in shoots, was markedly enhanced on NH_4^+ (Fig. 4F). These results suggest that AMOT1/EIN3 plays an important role in the NH_4^+-induced impairment of shoot growth. It was demonstrated furthermore that this inhibitory effect is related to enhanced shoot ACC and ethylene accumulation. More importantly, it was found that AMOT1/EIN3 positively regulates shoot ROS accumulation, which leads to oxidative stress in Arabidopsis shoots under NH_4^+ stress, and up-regulates the shoot expression of the genes coding for PODs previously shown to correlate positively with NH_4^+-induced increases in ROS content and cell growth inhibition (Podgórska *et al.*, 2015).

A role for ethylene evolution has long been suggested under NH_4^+ excess (Barker and Corey, 1991; Barker, 1999*a*, *b*), but its involvement remains incompletely understood. The present data indicate that ethylene evolution increases linearly with NH_4^+ treatment time (Fig. 4B), consistent with previous reports (Barker 1999*b*). Foliar ethylene evolution increased sharply in tomato when foliar NH_4^+ accumulation passed a critical value (Barker, 1999*a*). Our present and previous data also link the stimulation of *EBS:GUS* activity to NH_4^+ exposure (G. Li *et al.*, 2013; Supplementary Fig. S5). The present data show that shoot NH_4^+ content increases linearly with

increased treatment time (Fig. 4A). Furthermore, a previous observation showed high ethylene evolution to correlate with high tissue NH_4^+ but to be independent of nitrogen form and pH regime (Feng and Barker, 1992*c*). Hence, together with previous reports, our study suggests that greatly increased shoot NH_4^+ content may be the intrinsic trigger leading to enhanced ethylene evolution under NH_4^+ stress. The rate-limiting step in ethylene biosynthesis lies in the production of ACC by ACS (Schellingen *et al.*, 2014). Shoot ACC amounts also increased linearly with NH_4^+ treatment time (Fig. 4C). Furthermore, we show here that *AtACS2*, *AtACS7*, *AtACS11*, and *AtACO2*, which encode ACS and ACO, the two key enzymes responsible for ethylene synthesis, are transcriptionally up-regulated by NH_4^+ treatment (Fig. 4D). Therefore, it is conceivable that the increased ACC biosynthesis resulting from up-regulation of ACS and ACO gene expression is involved in NH_4^+-induced

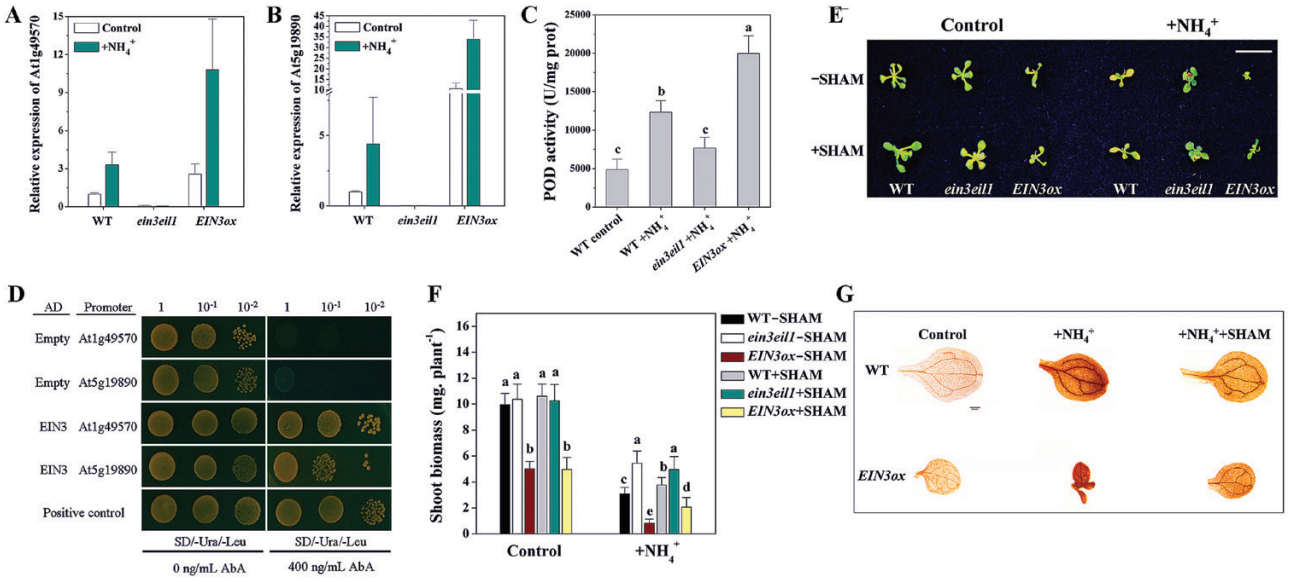

Fig. 7. EIN3 increases activity of PODs through transcriptional regulation of POD genes. (A and B) qRT-PCR analysis of the expression of two POD genes (At5g19890 and At1g48570) in WT, *EIN3ox*, and *ein3eil1* shoot tissue after NH_4^+ treatment for 6 h. Values are means ±SD of three replicates. *ACTIN2* was used as the internal reference gene, and the WT control was considered as 1. (C) Measurement of POD activity of WT, *EIN3ox*, and *ein3eil1* shoot tissue. Seedlings were exposed to 40 mM NH_4^+ for 5 d. Values are means ±SD of three replicates. (D) Y1H assay showing the EIN3 binding to the promoter of the two POD genes. The yeast expression plasmid pGADT7-EIN3 was reintroduced into the yeast strain Y1H Gold carrying the pAbAi-At1g49570 or pAbAi-At5g19890 vectors. The transformants (with or without dilutions) were screened for their growth on yeast synthetic defined medium (SD/-Ura -Leu) in the presence of 400 ng ml^{-1} AbA (antibiotic) for stringent selection. The empty vectors pGADT7 and p53-AbAi/pGAD-p53 were used as a negative and positive control, respectively. (E and F) Effect of salicylhydroxamic acid (SHAM) on the shoot biomass of the WT, *EIN3ox*, and *ein3eil1*. Five-day-old seedlings were transferred to medium alone or in combination with 10 μM SHAM for 6 d. A photograph of representative seedlings is shown in (E). Scale bars=1 cm. The shoot biomass is shown in (F). Values are the means ±SD, n=12. Different letters indicate statistical differences at P<0.05 of control and NH_4^+ treatment, respectively (one-way ANOVA with Duncan post-hoc test). (G) Effect of SHAM on the NH_4^+-induced H_2O_2 accumulation in shoots of WT and *EIN3ox*. Seedlings at 5 d were exposed to 40 mM NH_4^+ with or without 10 μM SHAM for 3 d, and then DAB staining of shoots was performed. Scale bars=200 μm.

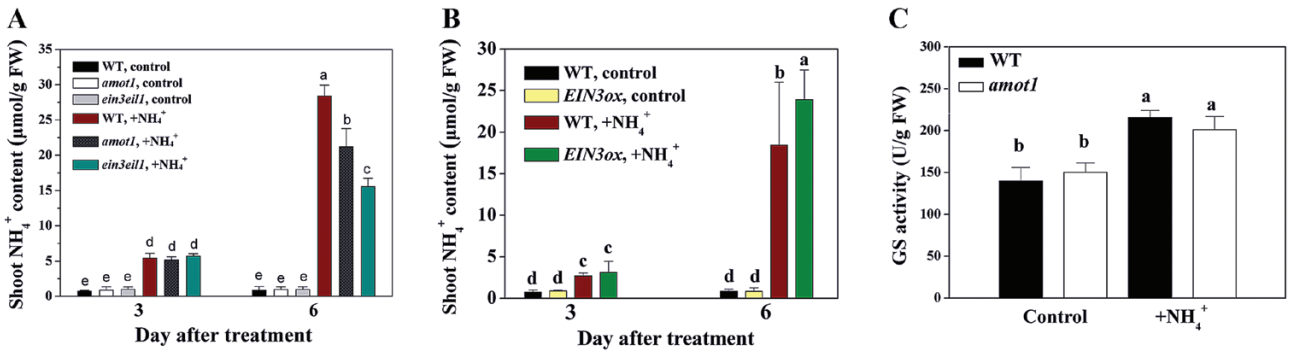

Fig. 8. Effects of NH_4^+ treatment on shoot NH_4^+ content and GS activity. (A) NH_4^+ contents in the shoot tissues of WT, *ein3eil1*, and *amot1* seedlings. Five-day-old WT, *ein3eil1*, and *amot1* seedlings were grown on growth medium and transferred to fresh medium with control or NH_4^+ for 3 d and 6 d of growth, and then NH_4^+ tissue content was determined. Values are means ±SD of three replicates. (B) NH_4^+ contents in the shoot tissues of WT and *EIN3ox* seedlings. Five-day-old WT and *EIN3ox* seedlings were grown on growth medium and transferred to fresh medium with control or NH_4^+ for 3 d and 6 d of growth, and then NH_4^+ tissue content was determined. Values are means ±SD of three replicates. (C) GS activities in the shoots of WT and *amot1* seedlings. Five-day-old WT and *amot1* seedlings were grown on growth medium and transferred to fresh medium with control or NH_4^+ for 6 d, and then GS activity was determined. Values are means ±SD of three replicates. Different letters indicate statistical differences at P<0.05 (one-way ANOVA with Duncan post-hoc test).

ethylene evolution. Further study on the detailed mechanisms of NH_4^+-regulated ethylene evolution is warranted.

In our study, we provide several lines of evidence supporting the notion that ethylene biosynthesis and signaling play a negative role in the adaptation of Arabidopsis shoot growth to NH_4^+ stress. ACC content, ethylene production, and AMOT1/EIN3 activity, and the expression of genes encoding key enzymes responsible for ethylene synthesis in the Arabidopsis shoot showed dramatic increases after NH_4^+ treatment. The dual evidence that shoot biomass was inhibited by NH_4^+ to a greater extent in the ethylene overproduction mutant *eto1-1* and the *EIN3ox* line, compared with the WT, and that mutations in ethylene receptors (e.g. *etr1-3*) and key positive regulators in ethylene signaling (e.g. *amot1* and *ein3-1*) showed increased shoot growth compared with the WT under NH_4^+ stress (Figs 3, 4H), supports this notion. The observations that the externally supplied ethylene inhibitor Ag^+ alleviated the phenotypic manifestation of toxicity, but that ACC, a precursor of ethylene, aggravated NH_4^+-suppressed shoot growth in the WT (Fig. 4E), further demonstrate the important role of shoot ethylene signaling. Our findings are in excellent agreement with a previous study showing that Ag^+ improved plant growth on NH_4^+ (Barker and Corey, 1991). Therefore, the data suggest that ethylene biosynthesis and signaling negatively regulate NH_4^+ tolerance of shoot growth in Arabidopsis.

The underlying mechanisms determining ROS accumulation by NH_4^+ in leaves are only partially understood (Bittsánszky *et al.*, 2015). Our results show that AMOT1/EIN3 is involved in H_2O_2 metabolism in leaves under NH_4^+ stress. First, a higher level of H_2O_2 cytochemical staining in *EIN3ox* was found, while a lower level of H_2O_2 staining was seen in *ein3eil1* than in the WT following NH_4^+ stress (Fig. 5A, B), in accordance with the NH_4^+ tolerance phenotypes and lipid peroxidation profiles of these genotypes (Figs 3, 6A). In agreement with the above results, NH_4^+ stress increased leaf H_2O_2 concentrations in the WT, while these were lower in *ein3eil1* and higher in *EIN3ox* under identical treatment conditions (Fig. 5C). Moreover, our split-shoot experiment showed that a higher DAB staining intensity was detected in the components of *EBS:GUS* cotyledons exposed to NH_4^+ (Supplementary Fig. S5). These results suggest that AMOT1/EIN3 positively regulates NH_4^+-induced leaf H_2O_2 accumulation. Investigations on whether oxidative stress is involved in NH_4^+ phytotoxicity have led to conflicting conclusions. The results of Domínguez-Valdivia *et al.* (2008) in spinach and pea suggest that stress originating from applying NH_4^+ as the only nitrogen source is not an oxidative stress. However, evidence is accumulating that NH_4^+ can induce oxidative stress in leaves, including in Arabidopsis (Podgórska and Szal, 2015), the aquatic plant *Hydrilla verticillata* (Wang *et al.*, 2010), and duckweed (Huang *et al.*, 2013). Our present results show that externally supplied H_2O_2 increases shoot growth sensitivity of *amot1* and *ein3eil1* to NH_4^+ stress (Fig. 6B). The extent of lipid peroxidation, estimated by monitoring the decomposition product MDA, has also been reported as elevated in NH_4^+-grown seedlings (Hachiya *et al.*, 2010; Podgórska *et al.*, 2013; Fig. 6A). Together, these findings indicate that increased H_2O_2 accumulation and oxidative stress in leaves under NH_4^+ stress at least partially result from elevated shoot AMOT1/EIN3 activity, providing a molecular basis for NH_4^+-induced accumulation of H_2O_2 in leaves. However, the present study shows that, although lower, there was still increased H_2O_2 accumulation and oxidative stress in *ein3eil1* mutant leaves under NH_4^+ stress (Figs 5, 6A), suggesting that there are pathways through which AMOT1/EIN3 functions independently to regulate shoot H_2O_2 accumulation and oxidative stress in response to NH_4^+ stress.

Drought can promote ROS biosynthesis by inducing expression of several *Atrboh* genes, such as *AtrbohA*, *AtrbohD*, and *AtrbohE* (Lee *et al.*, 2012). However, Podgórska *et al.* (2015) found that expression of the RBOHD gene is not induced in leaves under NH_4^+ stress. In this study, we show that there is no increase in RBOHA, RBOHB, RBOHD, or RBOHF expression in NH_4^+-treated WT, *EIN3ox*, and *ein3eil1* leaves. These results suggest that AMOT1/EIN3 is not involved through modulating expression of *Atrboh* genes under high NH_4^+, such as RBOHA, RBOHB, RBOHD, and RBOHF. However, we cannot exclude NADPH oxidase as a potential ROS source in NH_4^+-treated plants, as other RBOH genes might be up-regulated. NH_4^+-mediated changes in apoplastic pH (Husted and Schjoerring, 1995) may induce ROS generation, possibly through the modulation of the activities of cell wall PODs (Lager *et al.*, 2010). Furthermore, under low-Pi conditions, increased POD activities also inhibited Arabidopsis root growth by regulating ROS levels and cell wall stiffening, and the POD inhibitor SHAM could restore root growth and reduce ROS accumulation under –Pi (Balzergue *et al.*, 2017). Podgórska *et al.* (2015) showed that higher POD levels positively correlate with NH_4^+-induced ROS content and cell growth inhibition. Consistent with this, by examining POD gene expression and POD activity under NH_4^+ conditions, we show that NH_4^+ stress increases expression of some POD genes (At5g19890 and At1g48570) and POD activity in WT shoots (Fig. 7A–C). Moreover, the peroxidase inhibitor SHAM could indeed alleviate NH_4^+-induced shoot ROS accumulation (Fig. 7G; Supplementary Fig. S9) and growth inhibition (Fig. 7E, F). This result, together with previous reports, confirms that NH_4^+ induces accumulation of ROS and suggests that POD expression and activity may play an important role. Our qRT-PCR analyses show that two POD genes (At5g19890 and At1g48570) were constitutively up-regulated in *EIN3ox* but down-regulated in the *ein3eil1* double mutant, regardless of NH_4^+ (Fig. 7A). Moreover, NH_4^+-induced POD activity was positively correlated with the expression of EIN3 genes, as shown for *ein3eil1* and *EIN3ox* seedlings (Fig. 7B). Further studies revealed that the key transcription factor AMOT1/EIN3 may directly target the two POD genes (At5g19890 and At1g48570), as the AMOT1/EIN3 protein could specifically bind to the promoters of the At5g19890 and At1g48570 genes, as revealed by the Y1H assay. Further supporting our finding of increased POD activity and DAB staining, indicating H_2O_2 accumulation in *EIN3ox*, the POD inhibitor SHAM was shown to enhance *EIN3ox* shoot growth and reduce DAB staining used to indicate H_2O_2 accumulation under NH_4^+ stress (Fig. 7; Supplementary Fig. S9). Collectively, these data indicate that the ethylene signaling-mediated NH_4^+

response of Arabidopsis shoot growth is brought about, at least partially, through POD genes (e.g. At5g19890 and At1g48570), via AMOT1/EIN3.

The accumulation of free shoot NH_4^+ is widely considered to be critical to the development of NH_4^+ toxicity (Gerendas *et al.*, 1997; Szczerba *et al.*, 2008). Because H_2O_2 accumulation was greater in WT shoots than in *ein3eil1*, but higher in *EIN3ox* than in the WT, after a 3 d treatment with high NH_4^+, we hypothesized that loss of function or overexpression of AMOT1/EIN3 may entail reduced or enhanced NH_4^+ content in the shoot at the 3 d treatment time, respectively. However, there was no difference in shoot NH_4^+ content between the WT, *amot1*, *ein3eil1*, and *EIN3ox* (Fig. 8A). These results further highlight that AMOT1/EIN3 plays an important role in regulating NH_4^+-induced shoot ROS accumulation and rules out that reduced shoot ROS accumulation during the early phase of exposure (within 3 d in our study) by loss of function of AMOT1/EIN3 resulted from reduced NH_4^+ content. However, a higher NH_4^+ content in *EIN3ox* and the WT, and a lower content in *amot1* and *ein3eil1* were observed following high-NH_4^+ stress for prolonged treatment times (6 d) (Fig. 8A, B). Our results indicate that GS activity was not affected by the mutation in *AMOT1/EIN3* (Fig. 8C), showing that GS is not responsible for the lower NH_4^+ accumulation in the *amot1* mutant. Alternatively, oxidative stress itself, induced by H_2O_2, can increase cellular NH_4^+ concentrations by inducing proteolytic activity (Sweetlove *et al.*, 2002). It is not clear how AMOT1/EIN3 mediates shoot NH_4^+ accumulation over longer periods of treatment, and more research is warranted to examine this.

In summary, we have identified and characterized a novel gene, *AMOT1/EIN3*, that controls shoot NH_4^+ sensitivity and propose a model for ethylene–AMOT1/EIN3 functions in shoot NH_4^+ sensitivity (Fig. 9). Our study shows the importance of EIN3 in shoot inhibition under high-NH_4^+ stress, providing strong genetic evidence in support of the role of the ethylene biosynthesis and signaling pathway in regulating shoot NH_4^+ sensitivity. Under NH_4^+ stress, ethylene is perceived and transduced, affecting the transcription factors EIN3/EIL and initiating the ethylene response. Additionally, our work highlights the roles of AMOT1/EIN3 in regulating ROS accumulation in Arabidopsis shoots under NH_4^+ stress. In the *ein3eil1* mutant, high-NH_4^+-induced ROS accumulation is reduced, which leads to reduced oxidative stress in the shoot. However, *EIN3ox* shoots accumulated more ROS and displayed higher sensitivity to NH_4^+ stress. Elucidation of this interaction between AMOT1/EIN3 and H_2O_2 signaling provides novel insight into our understanding on how EIN3 regulates shoot growth under high-NH_4^+ stress. Moreover, it was found that AMOT1/EIN3 can up-regulate shoot expression of the genes coding for PODs (e.g. At5g19890 and At1g48570) previously shown to correlate positively with NH_4^+-induced ROS accumulation and cell growth inhibition. Further studies using molecular approaches to investigate the transcriptional network regulated by AMOT1/EIN3 will provide important new insights into the process of acclimation and of adaptation to NH_4^+ stress in plants.

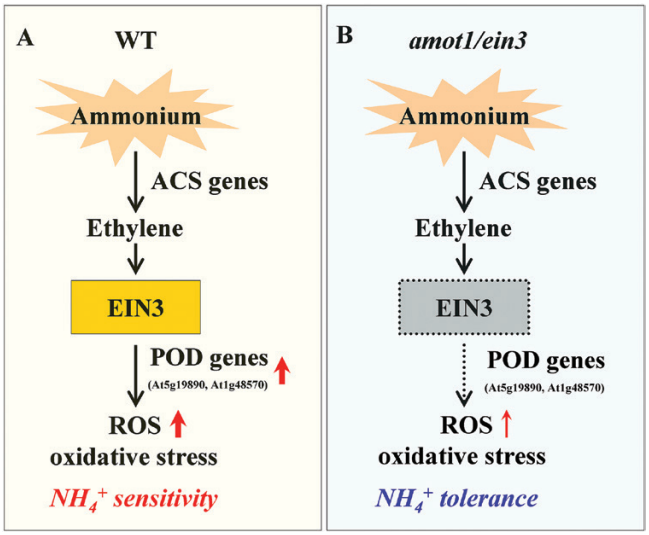

Fig. 9. A proposed model for ethylene–EIN3 function in shoot NH_4^+ sensitivity. Based on our study and previous reports (Chao *et al.*, 1997; G. Li *et al.*, 2013; Podgorska *et al.*, 2013, 2015), we established a model for ethylene–EIN3 function in shoot NH_4^+ sensitivity. (A) In the wild type, NH_4^+ stress enhanced the expression of *ACS* and *ACO* genes, encoding ACS and ACO, the two key enzymes responsible for ethylene synthesis. Under NH_4^+ stress, ethylene is perceived and transduced, affecting the transcription factor EIN3, and initiating the ethylene response. EIN3 regulates ROS accumulation, which leads to oxidative stress in Arabidopsis shoots under NH_4^+ stress. The expression of EIN3-mediated POD genes (e.g. At5g19890 and At1g48570) is involved in NH_4^+ stress-induced shoot ROS accumulation. (B) In the *amot1/ein3* mutant, expression of the AMOT1/EIN3-dependent POD genes (e.g. At5g19890 and At1g48570) in the shoot is blocked under NH_4^+ stress. Ethylene regulation of ROS accumulation and oxidative stress is lowered. Orthogons in orange represent known EIN3 functions, and orthogons in gray with dashed lines represent the inhibition of EIN3 functions due to the *amot1/ein3* mutation. Red arrows indicate increased POD gene expression, ROS accumulation, and oxidative stress, and thick and thin red arrows indicate, respectively, a high or low ROS accumulation and oxidative stress.

Supplementary data

Supplementary data are available at *JXB* online.

Fig. S1. Rosette diameter and fresh shoot weight of *Arabidopsis thaliana* wild-type (WT, Col-0) plants following treatment with various NH_4^+ concentrations.

Fig. S2. Relative rosette diameter (A) and fresh shoot weight (B) of *Arabidopsis thaliana* WT and *eil1* mutant plants following treatment with NH_4^+ for 6 d.

Fig. S3. Lateral root number of *Arabidopsis thaliana* WT and *ein3eil1* mutant plants following treatment with high NH_4^+ for 6 d.

Fig. S4. H_2O_2 content in WT, *EIN3ox*, and *ein3eil1* shoot tissue under control conditions.

Fig. S5. *EBS:GUS* expression and DAB staining in the split-shoot experiment.

Fig. S6. Effect of NH_4^+ treatment on shoot DAB staining and biomass of the WT and the *Atrbohd* mutant.

Fig. S7. qRT-PCR analysis of POD gene expression in WT, *EIN3ox*, and *ein3eil1* shoot tissue under NH_4^+ treatment for 6 h.

Fig. S8. Measurement of POD activity of WT, *EIN3ox*, and *ein3eil1* shoot tissue under control conditions.

Fig. S9. Mean relative DAB staining intensity in WT (A) and *EIN3ox* (B) shoots treated with NH_4^+ and NH_4^+ plus SHAM.

Table S1. Gene-specific primers used for qRT-PCR.

Acknowledgements

We thank Dr J. Alonso at North Carolina State University for providing seeds of the *EBS:GUS* reporter lines which were generated by Dr Anna Stepanova in Dr Joe Ecker's lab. We thank Dr Hongwei Guo for providing the seeds of *ein3-1*, *eil1-1*, *ein3eil1*, and *EIN3ox* transgenic lines, and the ABRC of Ohio State University for *etr1-3*, *eto1-1*, and *rbohd* mutant seeds. This work was supported by the National Natural Science Foundation of China (no. 31430095), the National Key R&D Program of China (no. 2017YFD0200103), the Chinese Academy of Sciences Innovation Program (no. CAS ISSASIP1604), and the University of Melbourne.

References

Adams DO, Yang SF. 1979. Ethylene biosynthesis: identification of 1-aminocyclopropane 1-carboxylic acid as an intermediate in the conversion of methionine to ethylene. Proceedings of the National Academy of Sciences, USA **76,** 170–174.

Alonso JM, Stepanova AN. 2004. The ethylene signaling pathway. Science **306,** 1513–1515.

Alonso JM, Stepanova AN, Solano R, Wisman E, Ferrari S, Ausubel FM, Ecker JR. 2003. Five components of the ethylene-response pathway identified in a screen for weak ethylene-insensitive mutants in *Arabidopsis*. Proceedings of the National Academy of Sciences, USA **100,** 2992–2997.

An F, Zhao Q, Ji Y, *et al*. 2010. Ethylene-induced stabilization of ETHYLENE INSENSITIVE3 and EIN3-LIKE1 is mediated by proteasomal degradation of EIN3 binding F-box 1 and 2 that requires EIN2 in *Arabidopsis*. The Plant Cell **22,** 2384–2401.

Apel K, Hirt H. 2004. Reactive oxygen species: metabolism, oxidative stress, and signal transduction. Annual Review of Plant Biology **55,** 373–399.

Balkos KD, Britto DT, Kronzucker HJ. 2010. Optimization of ammonium acquisition and metabolism by potassium in rice (*Oryza sativa* L. cv. IR-72). Plant, Cell & Environment **33,** 23–34.

Balzergue C, Dartevelle T, Godon C, *et al*. 2017. Low phosphate activates STOP1-ALMT1 to rapidly inhibit root cell elongation. Nature Communications **8,** 15300.

Barker AV. 1999*a*. Ammonium accumulation and ethylene evolution by tomato infected with root-knot nematode and grown under different regimes of plant nutrition. Communications in Soil Science and Plant Analysis **30,** 175–182.

Barker AV. 1999*b*. Foliar ammonium accumulation as an index of stress in plants. Communications in Soil Science and Plant Analysis **30,** 167–174.

Barker AV, Corey KA. 1991. Interrelations of ammonium toxicity and ethylene action in tomato. Hortscience **26,** 177–180.

Bindschedler LV, Dewdney J, Blee KA, *et al*. 2006. Peroxidase-dependent apoplastic oxidative burst in Arabidopsis required for pathogen resistance. The Plant Journal **47,** 851–863.

Bittsánszky A, Pilinszky K, Gyulai G, Komives T. 2015. Overcoming ammonium toxicity. Plant Science **231,** 184–190.

Bolwell GP, Davies DR, Gerrish C, Auh CK, Murphy TM. 1998. Comparative biochemistry of the oxidative burst produced by rose and French bean cells reveals two distinct mechanisms. Plant Physiology **116,** 1379–1385.

Britto DT, Kronzucker HJ. 2002. NH_4^+ toxicity in higher plants: a critical review. Journal of Plant Physiology **159,** 567–584.

Cao Y, Glass AD, Crawford NM. 1993. Ammonium inhibition of Arabidopsis root growth can be reversed by potassium and by auxin resistance mutations aux1, axr1, and axr2. Plant Physiology **102,** 983–989.

Chao Q, Rothenberg M, Solano R, Roman G, Terzaghi W, Ecker JR. 1997. Activation of the ethylene gas response pathway in *Arabidopsis* by the nuclear protein ETHYLENE-INSENSITIVE3 and related proteins. Cell **89,** 1133–1144.

Chen G, Bi YR, Li N. 2005. EGY1 encodes a membrane-associated and ATP-independent metalloprotease that is required for chloroplast development. The Plant Journal **41,** 364–375.

Coskun D, Britto DT, Li M, Becker A, Kronzucker HJ. 2013. Rapid ammonia gas transport accounts for futile transmembrane cycling under NH_3/NH_4^+ toxicity in plant roots. Plant Physiology **163,** 1859–1867.

Davletova S, Rizhsky L, Liang H, Shengqiang Z, Oliver DJ, Coutu J, Shulaev V, Schlauch K, Mittler R. 2005. Cytosolic ascorbate peroxidase 1 is a central component of the reactive oxygen gene network of *Arabidopsis*. The Plant Cell **17,** 268–281.

Domínguez-Valdivia MD, Aparicio-Tejo PM, Lamsfus C, Cruz C, Martins-Loução MA, Moran JF. 2008. Nitrogen nutrition and antioxidant metabolism in ammonium-tolerant and -sensitive plants. Physiologia Plantarum **132,** 359–369.

Dong CH, Zolman BK, Bartel B, Lee BH, Stevenson B, Agarwal M, Zhu JK. 2009. Disruption of Arabidopsis CHY1 reveals an important role of metabolic status in plant cold stress signaling. Molecular Plant **2,** 59–72.

Dupre C, Stevens CJ, Ranke T, Bleeker A, Peppler-Lisbach C, Gowing DJG, Dise NB, Dorland E, Bobbink R, Diekmann M. 2009. Changes in species richness and composition in European acidic grasslands over the past 70 years: the contribution of cumulative atmospheric nitrogen deposition. Global Change Biology **16,** 344–357.

Feng J, Barker AV. 1992*a*. Ethylene evolution and ammonium accumulation by nutrient-stressed tomato plants. Journal of Plant Nutrition **15,** 137–153.

Feng J, Barker AV. 1992*b*. Ethylene evolution and ammonium accumulation by nutrient-stressed tomatoes grown with inhibitors of ethylene synthesis or action. Journal of Plant Nutrition **15,** 155–167.

Feng J, Barker AV. 1992*c*. Ethylene evolution and ammonium accumulation by tomato plants with various nitrogen forms and regimes of acidity. I. Journal of Plant Nutrition **15,** 2457–2469.

Gerendas J, Zhu Z, Bendixen R, Ratcliffe RG, Sattelmacher B. 1997. Physiological and biochemical processes related to ammonium toxicity in higher plants. Zeitschrift für Pflanzenernährung und Bodenkunde **160,** 239–251.

Guo H, Ecker JR. 2004. The ethylene signaling pathway: new insights. Current Opinion in Plant Biology **7,** 40–49.

Guzmán P, Ecker JR. 1990. Exploiting the triple response of *Arabidopsis* to identify ethylene-related mutants. The Plant Cell **2,** 513–523.

Hachiya T, Watanabe CK, Boom C, Tholen D, Takahara K, Kawai-Yamada M, Uchimiya H, Uesono Y, Terashima I, Noguchi K. 2010. Ammonium-dependent respiratory increase is dependent on the cytochrome pathway in *Arabidopsis thaliana* shoots. Plant, Cell & Environment **33,** 1888–1897.

He W, Brumos J, Li H, *et al*. 2011. A small-molecule screen identifies L-kynurenine as a competitive inhibitor of TAA1/TAR activity in ethylene-directed auxin biosynthesis and root growth in Arabidopsis. The Plant Cell **23,** 3944–3960.

Hirano T, Satoh Y, Ohki A, Takada R, Arai T, Michiyama H. 2008. Inhibition of ammonium assimilation restores elongation of seminal rice roots repressed by high levels of exogenous ammonium. Physiologia Plantarum **134,** 183–190.

Huang L, Lu YY, Gao X, Du G, Ma XX, Liu M, Guo JS, Chen YP. 2013. Ammonium-induced oxidative stress on plant growth and antioxidative response of duckweed (*Lemna minor* L.). Ecological Engineering **58,** 355–362.

Husted S, Schjoerring JK. 1995. Apoplastic pH and ammonium concentration in leaves of *Brassica napus* L. Plant Physiology **109,** 1453–1460.

Jadid N, Mialoundama AS, Heintz D, *et al*. 2011. DOLICHOL PHOSPHATE MANNOSE SYNTHASE1 mediates the biogenesis of isoprenyl-linked glycans and influences development, stress response, and ammonium hypersensitivity in *Arabidopsis*. The Plant Cell **23,** 1985–2005.

Kim MJ, Ciani S, Schachtman DP. 2010. A peroxidase contributes to ROS production during *Arabidopsis* root response to potassium deficiency. Molecular Plant **3,** 420–427.

Kronzucker HJ, Siddiqi MY, Glass A. 1995. Analysis of $^{13}NH_4^+$ efflux in spruce roots (a test case for phase identification in compartmental analysis). Plant Physiology **109,** 481–490.

Kronzucker HJ, Siddiqi MY, Glass ADM. 1997. Conifer root discrimination against soil nitrate and the ecology of forest succession. Nature **385,** 59–61.

Lager I, Andréasson O, Dunbar TL, Andreasson E, Escobar MA, Rasmusson AG. 2010. Changes in external pH rapidly alter plant gene expression and modulate auxin and elicitor responses. Plant, Cell & Environment **33,** 1513–1528.

Lee S, Seo PJ, Lee HJ, Park CM. 2012. A NAC transcription factor NTL4 promotes reactive oxygen species production during drought-induced leaf senescence in *Arabidopsis*. The Plant Journal **70,** 831–844.

Lei G, Shen M, Li ZG, *et al*. 2011. EIN2 regulates salt stress response and interacts with a MA3 domain-containing protein ECIP1 in *Arabidopsis*. Plant, Cell & Environment **34,** 1678–1692.

Li B, Li Q, Su Y, Chen H, Xiong L, Mi G, Kronzucker HJ, Shi W. 2011. Shoot-supplied ammonium targets the root auxin influx carrier AUX1 and inhibits lateral root emergence in *Arabidopsis*. Plant, Cell & Environment **34,** 933–946.

Li B, Li Q, Xiong L, Kronzucker HJ, Krämer U, Shi W. 2012. *Arabidopsis* plastid AMOS1/EGY1 integrates abscisic acid signaling to regulate global gene expression response to ammonium stress. Plant Physiology **160,** 2040–2051.

Li BH, Li GJ, Kronzucher HJ, Baluška F, Shi WM. 2014. Ammonium stress in *Arabidopsis*: physiological targets, genetic loci, and signaling pathways. Trends in Plant Science **19,** 107–114.

Li G, Dong G, Li B, Li Q, Kronzucker HJ, Shi W. 2012. Isolation and characterization of a novel ammonium overly sensitive mutant, *amos2*, in *Arabidopsis thaliana*. Planta **235,** 239–252.

Li G, Li B, Dong G, Feng X, Kronzucker HJ, Shi W. 2013. Ammonium-induced shoot ethylene production is associated with the inhibition of lateral root formation in *Arabidopsis*. Journal of Experimental Botany **64,** 1413–1425.

Li Z, Peng J, Wen X, Guo H. 2013. Ethylene-insensitive3 is a senescence-associated gene that accelerates age-dependent leaf senescence by directly repressing *miR164* transcription in *Arabidopsis*. The Plant Cell **25,** 3311–3328.

Mittler R, Vanderauwera S, Gollery M, Van Breusegem F. 2004. Reactive oxygen gene network of plants. Trends in Plant Science **9,** 490–498.

Peng J, Li Z, Wen X, Li W, Shi H, Yang LS, Zhu HQ, Guo HW. 2014. Salt-induced stabilization of EIN3/EIL1 confers salinity tolerance by deterring ROS accumulation in *Arabidopsis*. PLoS Genetics **10,** e1004664.

Podgórska A, Gieczewska K, Łukawska-Kuźma K, Rasmusson AG, Gardeström P, Szal B. 2013. Long-term ammonium nutrition of *Arabidopsis* increases the extrachloroplastic NAD(P)H/NAD(P)$^+$ ratio and mitochondrial reactive oxygen species level in leaves but does not impair photosynthetic capacity. Plant, Cell & Environment **36,** 2034–2045.

Podgórska A, Ostaszewska M, Gardeström P, Rasmusson AG, Szal B. 2015. In comparison with nitrate nutrition, ammonium nutrition increases growth of the frostbite1 *Arabidopsis* mutant. Plant, Cell & Environment **38,** 224–237.

Podgórska A, Szal B. 2015. The role of reactive oxygen species under ammonium nutrition. In: Gupta KJ, Igamberdiev AU, eds. Reactive oxygen and nitrogen species signaling and communication in plants.Switzerland: Springer International Publishing, 133–153.

Qin C, Qian W, Wang W, Wu Y, Yu C, Jiang X, Wang D, Wu P. 2008. GDP-mannose pyrophosphorylase is a genetic determinant of ammonium sensitivity in *Arabidopsis thaliana*. Proceedings of the National Academy Sciences, USA **105,** 18308–18313.

Ren C, Zhang Y, Cui W, Lu G, Wang Y, Gao H, Huang L, Mu Z. 2015. A polysaccharide extract of mulberry leaf ameliorates hepatic glucose metabolism and insulin signaling in rats with type 2 diabetes induced by high fat-diet and streptozotocin. International Journal of Biological Macromolecules **72,** 951–959.

Rodrigues A, Santiago J, Rubio S, Saez A, Osmont KS, Gadea J, Hardtke CS, Rodriguez PL. 2009. The short-rooted phenotype of the brevis radix mutant partly reflects root abscisic acid hypersensitivity. Plant Physiology **149,** 1917–1928.

Sagi M, Fluhr R. 2006. Production of reactive oxygen species by plant NADPH oxidases. Plant Physiology **141,** 336–340.

Solano R, Stepanova A, Chao Q, Ecker JR. 1998. Nuclear events in ethylene signaling: a transcriptional cascade mediated by ETHYLENE-INSENSITIVE3 and ETHYLENE-RESPONSE-FACTOR1. Genes & Development **12,** 3703–3714.

Schellingen K, Van Der Straeten D, Vandenbussche F, Prinsen E, Remans T, Vangronsveld J, Cuypers A. 2014. Cadmium-induced ethylene production and responses in *Arabidopsis thaliana* rely on ACS2 and ACS6 gene expression. BMC Plant Biology **14,** 214.

Stepanova AN, Yun J, Likhacheva AV, Alonso JM. 2007. Multilevel interactions between ethylene and auxin in *Arabidopsis* roots. The Plant Cell **19,** 2169–2185.

Sweetlove LJ, Heazlewood JL, Herald V, Holtzapffel R, Day DA, Leaver CJ, Millar AH. 2002. The impact of oxidative stress on *Arabidopsis* mitochondria. The Plant Journal **32,** 891–904.

Szczerba MW, Britto DT, Balkos KD, Kronzucker HJ. 2008. Alleviation of rapid, futile ammonium cycling at the plasma membrane by potassium reveals K^+-sensitive and -insensitive components of NH_4^+ transport. Journal of Experimental Botany **59,** 303–313.

Tao JJ, Chen HW, Ma B, Zhang WK, Chen SY, Zhang JS. 2015. The role of ethylene in plants under salinity stress. Frontiers in Plant Science **6,** 1059.

Veljovic-Jovanovic S, Noctor G, Foyer CH. 2002. Are leaf hydrogen peroxide concentrations commonly overestimated? The potential influence of artefactual interference by tissue phenolics and ascorbate. Plant Physiology and Biochemistry **40,** 501–507.

Wang C, Zhang SH, Wang PF, Hou J, Li W, Zhang WJ. 2008. Metabolic adaptations to ammonia-induced oxidative stress in leaves of the submerged macrophyte *Vallisneria natans* (Lour.) Hara. Aquatic Toxicology **87,** 88–98.

Wang C, Zhang SH, Wang PF, Li W, Lu J. 2010. Effects of ammonium on the antioxidative response in *Hydrilla verticillata* (L.f.) Royle plants. Ecotoxicology and Environmental Safety **73,** 189–195.

Weigel D, Glazebrook J. 2002. How to study gene expression. In: Weigel D, Glazebrook J, eds. Arabidopsis: a laboratory manual. Cold Spring Harbor, NY: Cold Spring Harbor Laboratory Press, 243–245.

Xing Y, Jia W, Zhang J. 2008. AtMKK1 mediates ABA-induced *CAT1* expression and H_2O_2 production via AtMPK6-coupled signaling in *Arabidopsis*. The Plant Journal **54,** 440–451.

Yamagami T, Tsuchisaka A, Yamada K, Haddon WF, Harden LA, Theologis A. 2003. Biochemical diversity among the 1-amino-cyclopropane-1-carboxylate synthase isozymes encoded by the *Arabidopsis* gene family. Journal of Biological Chemistry **278,** 49102–49112.

Yoo SD, Cho Y, Sheen J. 2009. Emerging connections in the ethylene signaling network. Trends in Plant Science **14,** 270–279.

You W, Barker AV. 2002. Herbicidal actions of root-applied glufosinate-ammonium on tomato plants. Journal of the American Society for Horticultural Science **127,** 200–204.

You W, Barker AV. 2005. Ethylene evolution and ammonium accumulation by tomato plants after root-applied glufosinate-ammonium treatment in the presence of ethylene inhibitors. Communications in Soil Science and Plant Analysis **35,** 1957–1965.

Zhao B, Tian M, An Q, Ye J, Guo JS. 2017. Characteristics of a heterotrophic nitrogen removal bacterium and its potential application on treatment of ammonium-rich wastewater. Bioresource Technology **226,** 46–54.

Zou N, Li B, Chen H, Su Y, Kronzucker HJ, Xiong L, Baluška F, Shi W. 2013. GSA-1/ARG1 protects root gravitropism in *Arabidopsis* under ammonium stress. New Phytologist **200,** 97–111.

Zou N, Li B, Dong G, Kronzucker HJ, Shi W. 2012. Ammonium-induced loss of root gravitropism is related to auxin distribution and *TRH1* function, and is uncoupled from the inhibition of root elongation in *Arabidopsis*. Journal of Experimental Botany **63,** 3777–3788.